

# Online Heat Pattern Estimation in a Shaft Furnace by Particle Filter Logic

Yoshinari Hashimoto, Kazuro Tsuda  
Instrument and Control Engineering Dept.  
JFE Steel Corp.,  
Kawasaki, Japan

Emails: {y-hashimoto@jfe-steel.co.jp, k-tsuda@jfe-steel.co.jp}

**Abstract**— In steel-making plants, there are many processes, such as the blast furnace, in which the internal state is not directly observable. Automation of such processes based on process visualization is an urgent issue. Because the number of sensors is limited, the state estimation utilizing partial sensor information is necessary. We developed a technique which visualizes the whole temperature distribution of a shaft furnace by combining the sensor information and a nonlinear model calculation. Assuming that the difference between the model calculation and actual data derives from the fluctuation of unknown parameters which cannot be measured online, the parameters are estimated by a particle filter. This way, a robust state estimation logic was established. This technique was implemented and evaluated in a ferro-coke pilot plant at JFE Steel Corporation. As a result, estimation accuracy improved by 30 % compared with the model calculation without the state estimation.

*Keywords-Particle Filter; Data Assimilation.*

## I. INTRODUCTION

In steel making plants, there are many processes, in which the internal state cannot be measured directly. Such processes are operated manually depending on the operator's ability and experience. Hence, the automation based on the process visualization is an urgent issue.

There have been many approaches to the visualization of internal state by physical model calculation. For instance, complicated models which take into account fluid motion, reaction, and heat transfer have been developed [1]. However, because these models employ fixed parameters, they cannot deal with the transient phenomena caused by fluctuation of unknown parameters of materials characteristics, and so on.

In order to adapt to such situations, many studies have attempted to assimilate the model calculation with the partial information from the sensors, and compensate for modeling errors. Examples of conventional techniques are the Kalman filter [2], which is based on a linear approximation of the model, and the particle filter with simplified models based on a lumped element approximation [3][4]. In the field of process control, there have been a small number of studies that retain the feature of the model, which directly reflects nonlinear and complicated phenomena as a distributed

element model, while making the best use of sensor information.

On the other hand, in the field of meteorology, there have been numerous studies of data assimilation in which large scale numerical simulations are assimilated with observation data. Data assimilation can be classified into sequential type and non-sequential type. The former includes the particle filter [5] and the ensemble Kalman filter [6]; an example of the latter is the adjoint method [7]. The former has the advantages that the implementation is relatively easy and probability distribution of the state variable can be obtained. In particular, the particle filter features robustness and a clear physical interpretation.

In this research, nonlinear models assuming various unknown parameters are calculated online, based on the concept of the particle filter. The weight of each model is updated with the degree of coincidence with the actual data, and the unknown parameters are estimated online. In this way, flexible modeling which can follow the plant change with a clear interpretation can be achieved.

The state estimation technique based on the particle filter as outlined above was implemented in a ferro-coke furnace at JFE steel. Ferro-coke is a mixture of coal and iron ore with the ratio of 7 : 3 [8]. Owing to the catalytic effect of metallic Fe, the coke gasification reaction starts at lower temperature, compared with normal coke [9]. This reduces the temperature of thermal reserve zone in blast furnace, enabling low coke ratio operation. The ferro-coke manufacturing process consists of mixing, molding, and coking. The target of this research is the heat pattern of a ferro-coke furnace during the coking process.

There are several constraints on the heat pattern of the furnace, such as the temperature rising rate, coking time, and cooling condition. For example, a higher rising rate enhances the fluidity of coal grain, resulting in better product strength. The holding time in coking zone should be controlled in order to improve the strength and reactivity.

In spite of the necessity of online control of heat pattern, the number of sensors is limited. In addition, unknown parameters exist in the process, such as the heat loss from the oven surface and the specific heat of the solid, which cannot be detected online. Therefore, a state estimation logic based

on online parameter estimation with a particle filter is a proper approach.

The framework of this paper is as follows. In Section 2, the mathematical modeling of the ferro-coke furnace and the design of the particle filter are explained. A simulation study of state estimation is presented in Section 3. An evaluation of the estimation accuracy in the actual operation in a pilot plant is explained in Section 4. Finally, we conclude this paper in Section 5.

## II. MODELING OF THE SHAFT FURNACE

### A. Outline of the ferro-coke furnace

The structure of the ferro-coke furnace at the pilot plant is shown in Figure 1. Several tuyeres for coking and cooling are arranged symmetrically. There are three kinds of tuyeres, which are termed low temperature tuyere, hot tuyere, and cooling tuyere. The low temperature tuyere is used to adjust the temperature rising rate. The holding time in coking zone is achieved by the hot tuyere. The cooling tuyere and discharge device are installed at the bottom of the furnace.

Ferro-coke briquette are charged from the top of the furnace, and heated up by the heat exchange between the solid and the gas. After the coking process near the hot tuyere, the final product is released from the bottom.

Thermocouples TI (1)-TI (5) are arranged on the oven wall, which can monitor the temperature continuously. The thermocouples TI (6)-TI (8) are embedded in a probe, which is inserted in the furnace at appropriate times.

### B. Mathematical modeling

For the visualization of temperature distribution, a transient 2D model was developed, which takes into account the reaction, the fluid motion, and heat transfer. The details of the model are as follows. The parameters are listed in Table 1. The coordinate x-y is defined in Figure 1. The material balance of the solid and the gas is presented as the continuity equation,

$$\frac{\partial u_g}{\partial x} + \frac{\partial v_g}{\partial y} = R, \quad (1)$$

$$\rho_s \frac{\partial v_s}{\partial y} = -R. \quad (2)$$

Here, two kinds of reactions were considered as listed in Table 2. One is the gasification of the volatile component of the coal, and the other is the reduction of the iron ore, and they were assumed to be irreversible reaction. The rate of the reactions was a function of solid temperature. For the momentum of the gas flow, Ergun's equation [1] was solved,

$$(G_1 + G_2 |u_g|) \mu_g = -\frac{\partial p_g}{\partial x} \quad (3)$$

$$(G_1 + G_2 |v_g|) \mu_g = -\frac{\partial p_g}{\partial y} \quad (4)$$

where

$$G_1 = 150 \left( \frac{1 - \varepsilon_g}{\varepsilon_g d_p} \right)^2 \frac{\mu_g}{\varepsilon_g \rho_g}, \quad G_2 = 1.75 \left( \frac{1 - \varepsilon_g}{\varepsilon_g d_p} \right) \frac{1}{\varepsilon_g^2 \rho_g}.$$

In the case of the solid, the flow was simplified as a vertical descent, as described by (2). Next, the heat transfer model was developed to express the heat exchange between the solid and the gas, and the reaction heat. It is noteworthy that the time evolution term of (5) is negligible, because the heat capacity of the gas is much smaller than that of the solid.

$$\rho_g C_g \frac{\partial T_g}{\partial t} + \frac{\partial (C_g u_g T_g)}{\partial x} + \frac{\partial (C_g v_g T_g)}{\partial y} = \alpha (T_s - T_g) + R \Delta H_R \eta_1 \quad (5)$$

$$\rho_s C_s \frac{\partial T_s}{\partial t} + \frac{\partial (\rho_s C_s v_s T_s)}{\partial y} = \alpha (T_g - T_s) + R \Delta H_R \eta_2 \quad (6)$$

TABLE I. PARAMETERS IN THE MODEL

Symbol	Notes	Dimension
$u_g$	Mass velocity of the gas (Horizontal component)	$[kg / m^2 \cdot s]$
$v_g$	Mass velocity of the gas (Vertical component)	$[kg / m^2 \cdot s]$
$\rho_s$	Density of the solid	$[kg / m^3]$
$v_s$	Velocity of the solid	$[m / s]$
$R$	Reaction rate	$[kg / m^3 \cdot s]$
$p_g$	Gas pressure	$[Pa]$
$T_g$	Gas temperature	$[K]$
$T_s$	Solid temperature	$[K]$
$C_g$	Specific heat of gas	$[J / kg \cdot K]$
$C_s$	Specific heat of solid	$[J / kg \cdot K]$
$\Delta H_R$	Reaction heat	$[J / kg]$
$\eta_1$	Reaction heat distribution rate (gas)	$[-]$
$\eta_2$	Reaction heat distribution rate (solid)	$[-]$
$T_{out}$	Atmosphere temperature	$[K]$
$h$	Heat radiation coefficient	$[J / m^2 \cdot s \cdot K]$
$\alpha$	Heat exchange coefficient between gas and solid	$[J / m^3 \cdot s \cdot K]$
$\varepsilon_g$	Void ratio	$[-]$
$d_p$	Diameter of the material	$[m]$
$\rho_g$	Density of gas	$[kg / m^3]$
$\mu_g$	Viscosity of gas	$[Pa \cdot s]$
$c_1$	Parameter of reaction	$[-]$
$c_2$	Parameter of reaction	$[-]$

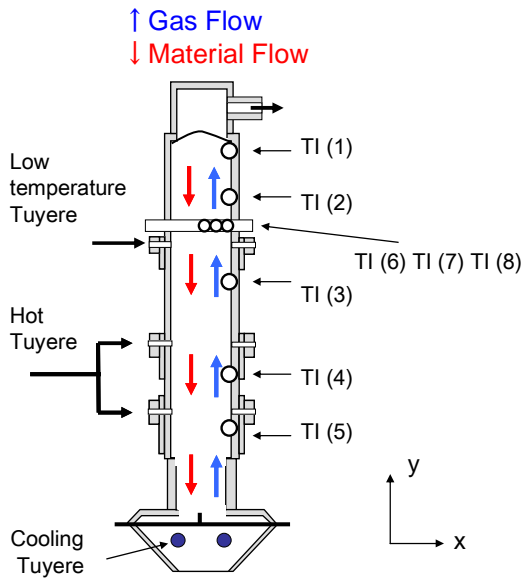


Figure 1. Structure of the ferro-coke furnace.

TABLE II. REACTIONS IN THE MODEL

Reaction	Notes	Dimension
$1/2\text{Fe}_2\text{O}_3 + 3/2\text{CO} \rightarrow \text{Fe} + 3/2\text{CO}_2$	$\frac{c_1}{1 + \exp(-(T_s - 600)/200)}$	$[\text{kmol} / \text{m}^3 \cdot \text{sec}]$
$\text{Coal(s)} \rightarrow \text{Coal(g)}$	$\frac{c_2}{1 + \exp(-(T_s - 400)/100)}$	$[\text{kg} / \text{m}^3 \cdot \text{sec}]$

The furnace wall was modeled as a boundary condition (7), where a heat exchange between the gas and the atmosphere occurs. This heat sink was incorporated in the gas heat calculation (5) as source term.

$$q = -h(T_g - T_{out}) \quad (7)$$

These differential equations are discretized by the finite volume method. The discretization scheme was Hybrid scheme [10]. The gas flow was solved by the SIMPLE algorithm, in which the pressure and the mass velocity are solved in a convergent calculation with (1), (3) and (4). Time marching was modeled by a first order implicit scheme. The time step was 10 minutes, considering the time-scale of the phenomenon in the furnace.

The discretized equations can be expressed in the form

$$\begin{aligned} &(\mathbf{T}_s(k+1), \mathbf{T}_g(k+1)) \\ &= f(\mathbf{T}_s(k), \mathbf{T}_g(k), \mathbf{u}(k), \mathbf{A}(k)) \end{aligned} \quad (8)$$

where  $\mathbf{T}_s(k)$ ,  $\mathbf{T}_g(k)$  are the temperature distribution of the solid and the gas at time step  $k$ , respectively,  $\mathbf{u}(k)$  is the model input, such as the inflow gas volume and temperature, and  $\mathbf{A}(k)$  is the set of unknown parameters, which were assumed to fluctuate.

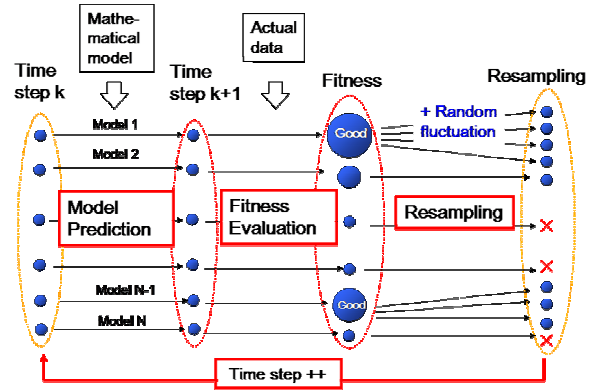


Figure 2. Algorithm of the particle filter.

Organizing the equations in this form is helpful when they are incorporated into the particle filter logic as described in Section 3.

### C. Algorithm of particle filter

In this section, the algorithm of the particle filter, which assimilates the sensor information and model calculation, is explained. Summarizing the logic, various models assuming different parameter are prepared, and the temperature distribution is calculated in parallel. Then, the fitness of each model with the actual data is evaluated by the actual sensor data, and the number of copies of the model for the next time step is determined by the fitness. As shown in Figure 2, the procedure consisting of model prediction, evaluation, and making copies is repeated at every time step.

This way, the accuracy of the model is retained. The details of the algorithm consist of five steps, as follows.

Step (1): As the initial guess of the unknown parameters, various sets of the parameters are prepared. Here, we assume that the fluctuating parameters are the specific heat of the solid, and the heat radiation coefficient of the furnace wall. Hereafter, each set of the unknown parameters is to be called "particle". The number of the particles was 25.

The weight of the particles was set to be equal, that is,

$$w_i(1) = 1/N \quad (9)$$

where  $w_i(k)$  is the weight of  $i$  th particle at time step  $k$ , and  $N$  is the number of particles.

Step (2): Based on the unknown parameters of each particle, the temperature distribution is predicted using the transient model as shown in (8),

$$\begin{aligned} &(\mathbf{T}_{s,i}(k), \mathbf{T}_{g,i}(k)) \\ &= f(\mathbf{T}_{s,i}(k-1), \mathbf{T}_{g,i}(k-1), \mathbf{u}(k-1), \mathbf{A}_i(k-1)) \end{aligned} \quad (10)$$

where  $\mathbf{T}_{s,i}(k)$  is the temperature distribution of the solid at time step  $k$ , and  $\mathbf{T}_{g,i}(k)$  is the temperature distribution of the solid at time step  $k$ , with respect to  $i$  th particle.

As this step is conducted independently for each particle, it is helpful to organize the transient model into the form as described in Section 2-B.

Step (3): The fitness between the actual data and the predicted temperature at the sensor locations is evaluated for each particle. First, the temperature prediction of the model of the  $i$  th particle at the sensor position can be obtained as,

$$\mathbf{y}_i(k) = \mathbf{C}\mathbf{T}_{g,i}(k) \quad (11)$$

where  $\mathbf{C}$  is the observation matrix, which extracts the value at the sensor positions from the calculated temperature distribution. In this case, we assumed that the thermocouples measure the temperature of the gas, because the thermocouples were embedded in the wall, and there was no direct contact with the material.

The definition of the fitness was defined as

$$\theta_i(k) = \exp\left(-\frac{|\mathbf{y}_i(k) - \mathbf{y}_{act}(k)|^2}{\sigma^2}\right) \quad (12)$$

where the suffix *act* means the actual value from the sensors, and  $\sigma$  is the assumed observation error of the sensors.

Step (4): The weight of each particle is updated with the fitness, based on Bayes' theorem [5].

$$w_i(k) \leftarrow w_i(k)\theta_i(k) \quad (13)$$

$$w_i(k) \leftarrow \frac{w_i(k)}{\sum_i w_i(k)}. \quad (14)$$

The weight  $w_i(k)$  is updated by multiplication by the fitness  $\theta_i(k)$ , and normalized so that the total weight is unity. The estimation of the unknown parameters and temperature distribution at time step  $k$  can be expressed as the weighted average of the particle.

Step (5): The copies of the particles are generated with the probability proportional to the weight of each particle. Thus, a particle with a larger weight has a greater chance of leaving more copies for the next time step. After that, the unknown parameters are slightly adjusted with random numbers to avoid making completely identical particles. In this case, an arbitrary number was selected from 0.995 to 1.005, and the unknown parameters were adjusted by multiplying the number. Then, the weight of each particle is set to be equal.

Online estimation of unknown parameters is possible by conducting Step (2)-Step (5) at each time step. Therefore, higher accuracy is achievable, compared with the calculation by fixed parameters.

### III. SIMULATION RESULT

This section describes a simulation study of the assimilation logic, as discussed in Section 2-C. Here, so called twin experiment was carried out as shown in Figure 3. In the virtual plant, the unknown parameters were changed dynamically. Then, using the particle filter, the partial temperature information at the sensor positions in the virtual plant was assimilated with the model calculation without sensing the fluctuation of the parameters. The performance

of the particle filter was checked by confirming that the change of the unknown parameters was identified properly, and that the temperature distribution of the virtual plant was estimated.

The unknown parameters are assumed to be the heat radiation coefficient of the oven surface and the specific heat of the solid. These parameters fluctuate in the virtual plant as shown in Figure 4.

The partial information of the temperature distribution at the sensor positions in Figure 1 was utilized as the input of the particle filter logic. The model input, such as the gas inflow temperature and volume are taken from the actual operation data of the pilot plant.

The estimation results of the surface temperature and the internal temperature are shown in Figure 5. The estimation with assimilation corresponds to the temperature visualization result by particle filter in Figure 3, and the estimation without assimilation means the mathematical model calculation without using sensor information in Figure 3. The temperature is scaled by the deviation from the set point. The temperatures of the virtual plant, the estimation result without the data assimilation, and the result with the assimilation are compared. The particle filter logic was set to be effective at time step 250. The upper two of the three rows are the results of the surface temperature, which are observable and used for the input of the particle filter. The bottom row is the result of the internal temperature, which is not observable. At all three positions, the estimated temperature gradually converges on the virtual plant data.

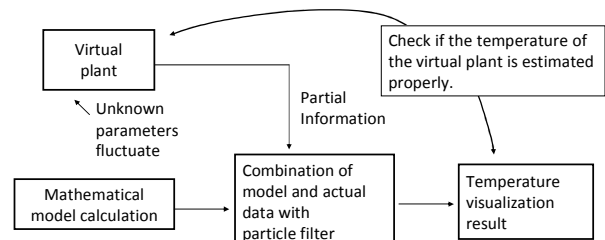


Figure 3. Validation of the particle filter by simulation.

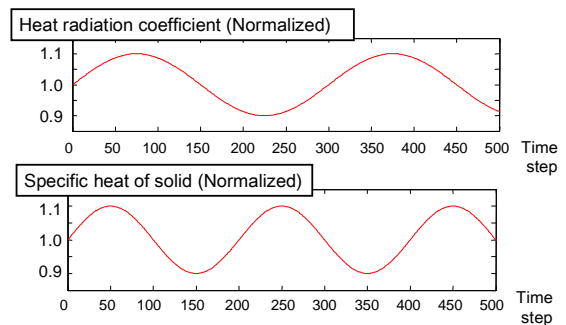


Figure 4. Assumed unknown parameters change.

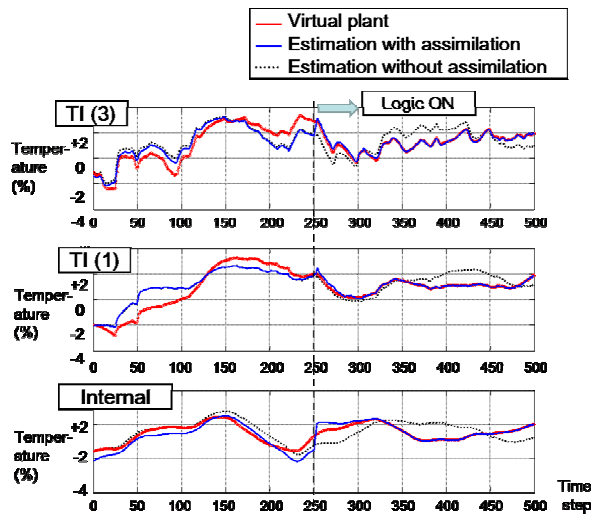


Figure 5. Estimation result of the temperature distribution.

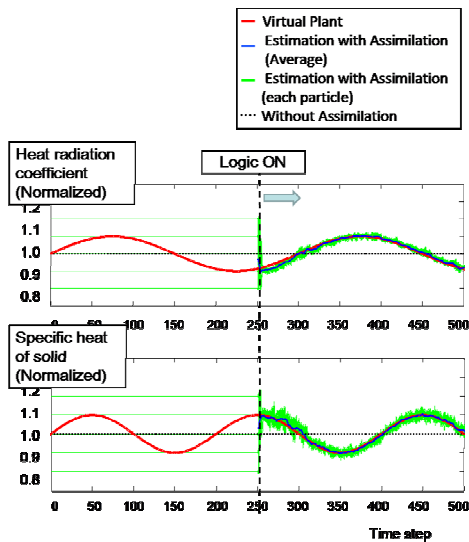


Figure 6. Result of parameter estimation by particle filter.

The result of parameter estimation is shown in Figure 6. The green lines show the result of 25 particles. It can be understood that each particle is searching the unknown parameters around the true value after applying the particle filter.

In this way, it was confirmed that the identification of the unknown parameters, and the estimation of the internal temperature, which cannot be measured online, are achievable with the particle filter logic.

#### IV. EVALUATION IN THE ACTUAL OPERATION

In this section, the validation result of the state estimation logic at an actual plant is presented. The particle filter logic was implemented at the operation room of a ferro-coke plant at JFE steel. Four of the five thermocouples, which are TI (1), TI (3), TI (4), TI (5) in Figure 1, were used for the input of

the particle filter. The remaining one, TI (2) was used for validation of the logic. As explained in Section 3, we assumed that the unknown parameters were heat radiation coefficient and specific heat of the solid. First, the estimation results of the thermocouples used as the input are shown in Figure 7. The temperature is scaled by the deviation from the set point. For the sake of comparison, this figure shows plots of not only the model calculation with the state estimation, but also the calculation without the assimilation logic, which was conducted offline. The estimation accuracy improved by more than 50 % on average by the assimilation.

Next, the result of the validation thermocouple is explained. This result is shown in Figure 8. Since estimation accuracy improved by 40%, an over-fitting problem does not occur in this case. The estimation result of the internal temperature, which are TI (6)-TI (8) in Figure 1, is presented in Figure 9, where the actual temperature was measured by the probe in Figure 1. The estimated temperature agreed well with the actual temperature. In this case, estimation accuracy improved by 30 %. In comparison with the case of surface temperature, the performance of the assimilation declines because of the phenomenon which cannot be expressed by the assumed unknown factors, such as the fluctuation of the reduction reaction rate. The reaction rate greatly depends on the coal grain size inside the Ferro-coke briquette which cannot be detected online. Another unknown factor is the heat exchange ratio between gas and solid, which is influenced by the shape of the briquette.

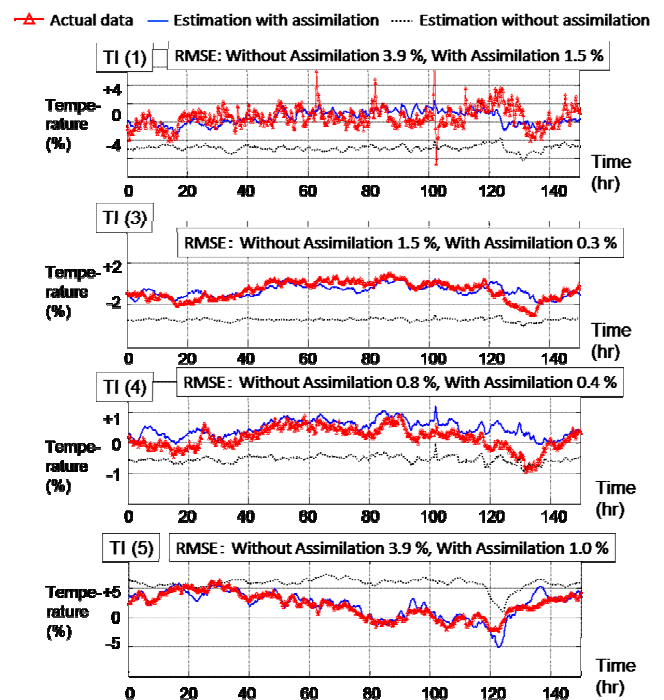


Figure 7. Estimation result of the temperature.

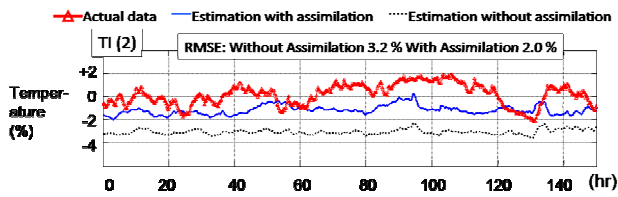


Figure 8. Temperature estimation at the validation point.

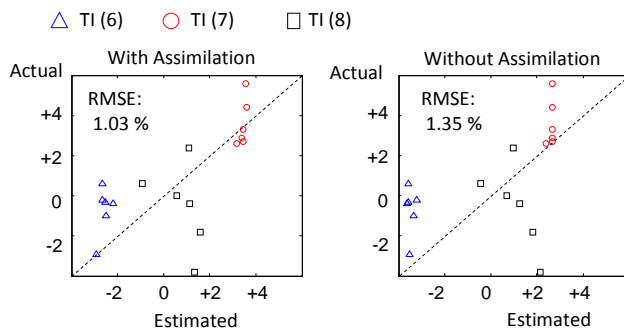


Figure 9. Estimation result of the internal temperature.

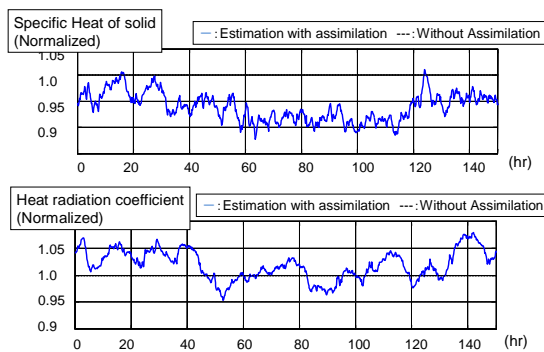


Figure 10. Estimation result of the unknown parameters.

The estimation result of the unknown parameters is shown in Figure 10. The blue line shows the estimation result, and the black dotted line shows the values of offline calculation with fixed parameters. The fluctuation of the specific heat reflects the type of material and the enthalpy of the reaction. The heat radiation coefficient changes due to the contact between the material and oven wall, and the condition of the oven surface.

In this way, the performance of the state estimation technique based on the particle filter was validated in the actual operation. The performance of the particle filter can be enhanced further by adding other unknown factors, such as heat exchange rate, reduction reaction rate, and so on. However, in such case, the number of the particles should be increased, and shortening the calculation time of the physical model is necessary. Considering the limit of the calculation time, identifying the unknown factors which mainly contribute to fluctuation of the temperature distribution in the

actual plant is the key element for the practical application of this method.

## V. CONCLUSION AND FUTURE WORK

In this research, online state estimation logic based on the particle filter logic was developed. An estimation logic of the whole temperature distribution of a shaft furnace was established by combining the partial sensor information and a nonlinear model calculation. The performance of the estimation logic was confirmed in a simulation study. As a result of an evaluation in actual operation, the estimation accuracy improved by more than 30 % compared with the model calculation without the state estimation.

As future work, the temperature control logic based on state estimation will be developed. The state estimation logic enables the control of inner temperature distribution of the furnace, which cannot be observed directly. Possible manipulated variables are the gas temperature or the gas volume of the tuyeres.

## REFERENCES

- [1] K. Takatani, T. Inada, and Y. Ujisawa, "Three - dimensional Dynamic Simulator for Blast Furnace," *ISIJ International*, vol. 39, 1999, pp. 15-22.
- [2] J. Brännbacka and H. Saxén, "Modeling the Liquid Levels in the Blast Furnace Hearth," *ISIJ International*, vol. 41, 2001, pp. 1131-1138.
- [3] S. Sonoda, N. Murata, H. Hino, H. Kitada, and M. Kano, "A Statistical Model for Predicting the Liquid Steel Temperature in Ladle and Tundish by Bootstrap Filter," *ISIJ International*, vol. 52, 2012, pp. 1086-1091.
- [4] N. Kaneko, S. Matsuzaki, M. Ito, H. Oogai, and K. Uchida, "Application of Improved Local Models of Large Scale Database-based Online Modeling to Prediction of Molten Iron Temperature of Blast Furnace," *ISIJ International*, vol. 50, 2010, pp. 939-945.
- [5] T. Higuchi, "Monte Carlo filter using the genetic algorithm operators," *Journal of Statistical Computation and Simulation*, vol. 59, 1997, pp. 1-23.
- [6] G. Ueno, T. Higuchi, T. Kagimoto, and N. Hirose, "Application of the ensemble Kalman filter and smoother to a coupled atmosphere-ocean model," *SOLA*, vol. 3, 2007, pp. 5-8.
- [7] M. Kano, S. Miyazaki, and K. Ito, "An adjoint data assimilation method for optimizing frictional parameters on the afterslip area," *Earth, Planets and Space*, vol. 65, 2013, pp. 1575-1580.
- [8] S. Nomura, H. Terashima, E. Sato, and M. Naito, "Some Fundamental Aspects of Highly Reactive Iron Coke Production," *Tetsu-to-Hagané*, vol. 92, no. 12, 2006, pp. 849-855.
- [9] S. Ueda, K. Yanagiya, K. Watanabe, T. Murakami, R. Inoue, and T. Ariyama, "Reaction Model and Reduction Behavior of Carbon Iron Ore Composite in Blast Furnace," *ISIJ International*, vol. 49, no. 6, 2009, pp. 827-836.
- [10] S.V.Patankar, *Numerical Heat Transfer and Fluid Flow*. Hemisphere: Washington DC/New York, 1980.